Applied Surface Science 255 (2008) 3400–3406

Contents lists available at ScienceDirect

Applied Surface Science

journal homepage: www.elsevier.com/locate/apsusc

Fabrication of poly(methyl methacrylate) colloidal monolayer on chemically modified silicon surface and hemispherical platinum nanoshell

Hye Jin Nam, Young-Uk Kwon, Duk-Young Jung *

Department of Chemistry-BK21, Institute of Basic Sciences, Sungkyunkwan Advanced Institute of NanoTechnology, Sungkyunkwan University, Suwon 440-746, Republic of Korea

ARTICLE INFO

Article history:
Received 18 August 2008
Received in revised form 22 September 2008
Accepted 22 September 2008
Available online 2 October 2008

PACS:
68. 43. Mn
81. 15. Cd
81. 16. Dn
82. 35. Gh

Keywords:
Colloidal crystal
Self-assembly
Surface modification
APTES
Platinum
Sputtering
Hemispherical nanoshell

ABSTRACT

A dip-coating technique was used to deposit self-assembled monolayer arrays of PMMA colloidal particles with a diameter of 125 nm onto a silicon surface coated with (3-aminopropyl)-triethoxysilane (APTES), exploiting the electrostatic interaction between the negative particle and the positive substrate. The PMMA colloidal arrangement was controlled efficiently by the dipping time and temperature, concentration and pH of the colloidal solutions. A non-close-packed monolayer assembly was prepared without the need for pre-patterned templates. The deposition of platinum metal on the 2D PMMA arrays and subsequent thermal treatment produced ordered hemispherical Pt nanoshells, 74 nm in height, as soft-lithographic templates and biological sensor materials.

1. Introduction

Ordered colloidal films of highly uniformed polymer or inorganic microspheres have attracted considerable attention due to the developments in areas related to nano-engineered structures, such as electrooptics [1], chemical and biological sensors [2,3], catalysis [4], and membranes [5]. The most valuable tool for constructing multi-dimensional structures from nano-sized materials is the 'bottom-up' self-assembly process of colloidal particles. Monodispersed colloidal particles can be readily self-assembled into a long-range ordered lattice forming 2D or 3D structured materials [6,7]. Therefore, there has been a great deal of research aimed at fabricating the homogeneous crystalline arrays with a well-defined structure, sufficiently large domain size and desirable film thickness.

The fabrication of highly ordered crystalline structures together with the development in areas of microengineering using lithographic techniques [8–10] has been achieved through the self-assembly of colloidal particles on pre-patterned structures, such as V-shaped grooves or square pyramidal fits, or other lithographic fabrics using conventional lithographic techniques [11,12]. However, the template-induced assembly has several shortcomings that require a photolithographically-patterned template, expensive equipment and complex fabrication processes for microfabrication. On the other hand, non-template techniques, for example dip-coating, are inexpensive, facile fabrication processes with the ability to control the particle aggregation and transport on solid surfaces using chemical modification. Chemical modification of a substrate using amine ($-NH_2$) or thiol (-SH) end groups to enhance the specific binding affinity is widely used to fabricate SAMs-based micro-and nano-structures [13,14]. Recently, there has been increasing attention focused on the binding affinity of organic molecules within the pore structure of mesoporous silica materials, such as MCM-41, 48 and SBA-15 [15].

* Corresponding author. Fax: +82 31 290 7075.
E-mail addresses: hj1227@skku.edu (H.J. Nam), ywkwon@skku.edu (Y.-U. Kwon), dyjung@skku.edu (D.-Y. Jung).

0169-4332/$ – see front matter © 2008 Elsevier B.V. All rights reserved.
doi:10.1016/j.apsusc.2008.09.057

An efficient colloidal assembly was exploited using the molecular linker, (3-aminopropyl)triethoxysilane (APTES), to form a stable interface between PMMA particles. Control of the interface is the most important technique in colloidal systems because the resulting structural features are affected greatly by both particle-particle and particle-substrate interactions [16]. APTES on a silicon substrate makes the silicon substrate surface hydrophilic, resulting in the preferred adsorption of colloidal particles. This paper suggests the optimized experimental conditions e.g., reaction time, temperature, concentration and pH of colloidal solutions, to produce ordered 2D monolayers of PMMA microspheres. The heat treatment of a platinum-PMMA composite produced a 2D array of uniform hemispherical Pt nanoshells by removing the PMMA template. This paper reports a facile and reproducible method for fabricating platinum nanoshells without the use of lithographically pre-patterned templates.

2. Experimental

2.1. Materials

All chemicals were purchased from Aldrich and were used as received. The deionized water was prepared from a Milli-Q-system (18.2 MΩ cm^{-1} in resistivity). The Si (1 0 0) substrate was cleaned before use under sonication in a freshly prepared piranha solution (3:1, H_2SO_4/H_2O_2 (35%)) to remove the residual organic impurities, followed by sonication for 30 min. The substrates were then rinsed with deionized water and isopropyl alcohol, and dried in a nitrogen stream. They were retreated with oxygen plasma using Harrick plasma cleaner operating at 30 W.

2.2. Preparation of PMMA beads

Soap-free emulsion polymerization technique was used to prepare monodisperse 125 nm PMMA colloidal particles [17] and carried out in a 250 mL three-neck round flask with thermometer, agitator and condenser. Briefly, 6.0 mL of the monomer and 6.0 mL of toluene were added dropwise to 60 mL of water at 90 °C under a nitrogen atmosphere for several minutes, and then heated at 90 °C for 1 h. 0.030 g of potassium persulfate radical initiator dissolved in 5.0 mL of water at 90 °C was then added to the solution under a nitrogen flow, and stirred for 25 min vigorously. The hot solution was opened to the air, and the resulting white dispersion was purified by air flow at 90 °C to remove the unreacted monomer and toluene. Finally, the PMMA colloidal solutions were separated by filtration, and purified by centrifugation four times. The particle sizes of the colloidal particles were measured to be 125 nm by SEM.

2.3. PMMA monolayer assembly

The surface of silicon substrate was treated with APTES, (3-aminopropyl)triethoxysilane to increase surface binding affinity of negatively charged PMMA particles on silicon substrate. Vacuum deposition of APTES was carried out at 1.0×10^{-3} torr for 10 min, which was followed by heat treatment at 100 °C for 10 min. After washing with 2-propanol, the APTES-coated silicon substrate was dipped into a 0.1 M HCl solution for 30 min, washed with copious amounts of water, and dried under a N_2 flow. For the kinetic study, four colloidal solutions with different concentrations and pH were prepared: Solution 1, PMMA stock solution with 1.2×10^7 particle and pH 5.6; Solution 2, 1/2 concentration of Solution 1 and pH 5.8; Solution 3, Solution 1 at pH 2.0; and Solution 4, Solution 1 at pH 3.0. The pH was controlled by adding a 0.1 M HCl solution. The PMMA-coated samples were prepared by dipping the substrates into each solution, followed by washing with deionized water and drying in air for 1 day. The substrates were dipped into the four solutions for 2 h, 8 h, 12 h and 18 h, respectively. The reaction temperatures used were 30 °C, 50 °C, 70 °C and 80 °C, respectively. For determination of the ratios of the substrate area covered by the PMMA particles to the total film area was determined by analyzing the scanning electron microscopy (SEM) images with dimensions of 12 μm × 9 μm. The average values of 20 samples were calculated. The hemispherical nanoshell was formed by depositing Pt metal to a thickness of 4 nm on the PMMA attached silicon substrate by sputtering followed by heating in a conventional oven at 250 °C for 1 h to remove the PMMA template.

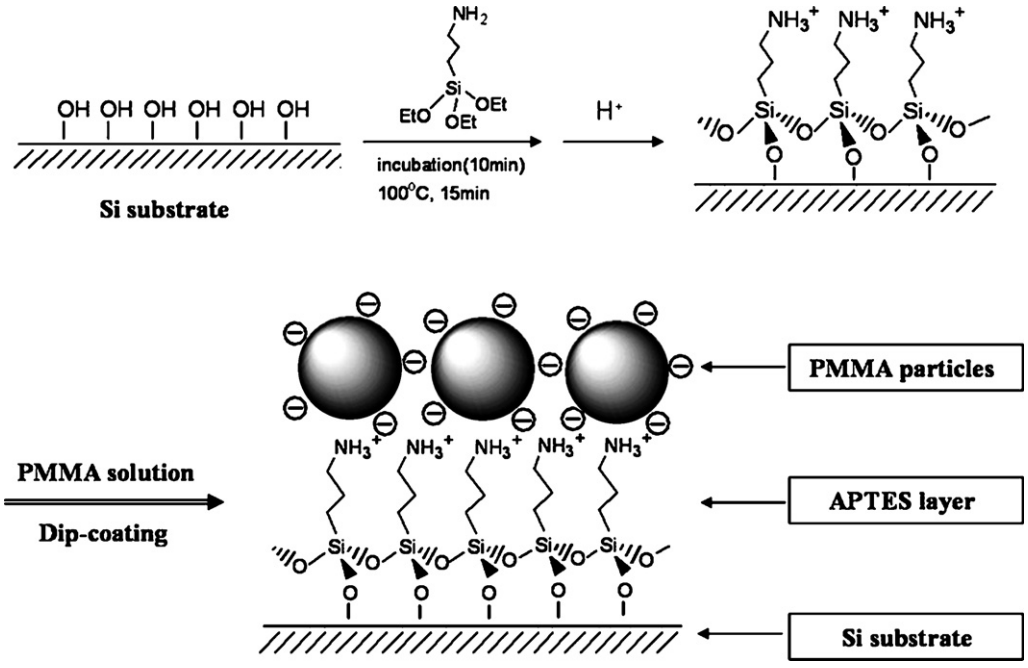

Fig. 1. Schematic procedures for producing the monolayer of PMMA particles on APTES-coated silicon substrate by dip-coating.

Table 1
Time-dependent surface coverage ratios (%) of the PMMA particles on the APTES-coated substrate for each colloidal solution at 20 °C.

Dip-coating time (h)	Surface coverage ratios (%)			
	Solution 1	Solution 2	Solution 3	Solution 4
2	19 ± 5	12 ± 1	45 ± 2	35 ± 3
8	21 ± 3	17 ± 2	49 ± 1	37 ± 2
12	23 ± 2	20 ± 2	50 ± 3	39 ± 2
18	25 ± 1	22 ± 1	52 ± 3	41 ± 1

Table 2
Temperature-dependent surface coverage ratios (%) of the PMMA particles on the APTES-coated substrate for each colloidal solution at elevated temperatures for 2 h.

Dip-coating temperature (°C)	Surface coverage ratios (%)			
	Solution 1	Solution 2	Solution 3	Solution 4
30	22 ± 1	22 ± 1	40 ± 1	34 ± 1
50	26 ± 2	24 ± 3	44 ± 3	38 ± 1
70	29 ± 1	26 ± 1	46 ± 1	40 ± 3
80	33 ± 2	28 ± 2	50 ± 3	42 ± 3

2.4. Characterization

The electrophoretic mobility of the obtained PMMA particles was measured using a Malvern Zetasizer 4 and the reported result is an average of four measurements. The ζ–potential was calculated by converting the electrophoretic mobility, μ, using the Smoluchowski relation: $\zeta = \mu\eta/\varepsilon$, where η and ε are the viscosity and permittivity of the solution, respectively [18]. The SEM images were taken on a JEOL JSM6700F at an accelerating voltage of 15 kV. Prior to the observations, the samples were sputtered with a thin platinum layer (3–4 nm thickness) using a 108 Auto Sputter Coater (Pelco inter, Co).

3. Results and discussion

3.1. PMMA colloidal monolayer

The monodisperse PMMA colloidal particles, 125 nm in size, were obtained from the emulsion polymerization of methylmethacrylate (MMA). The zeta potential of the prepared PMMA colloidal solution had a negative surface potential of −50 mV, presumably due to the termination of the polymer surface by the sulfate group

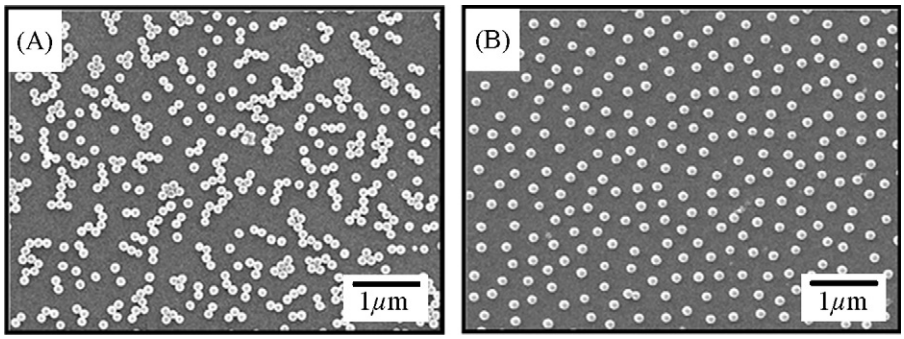

Fig. 2. SEM images of the APTES-coated substrate in the solution 1 (A) and solution 2 (B) at room temperature showing the concentration-dependent monolayer assembly of PMMA spheres obtained at 20 °C for 2 h.

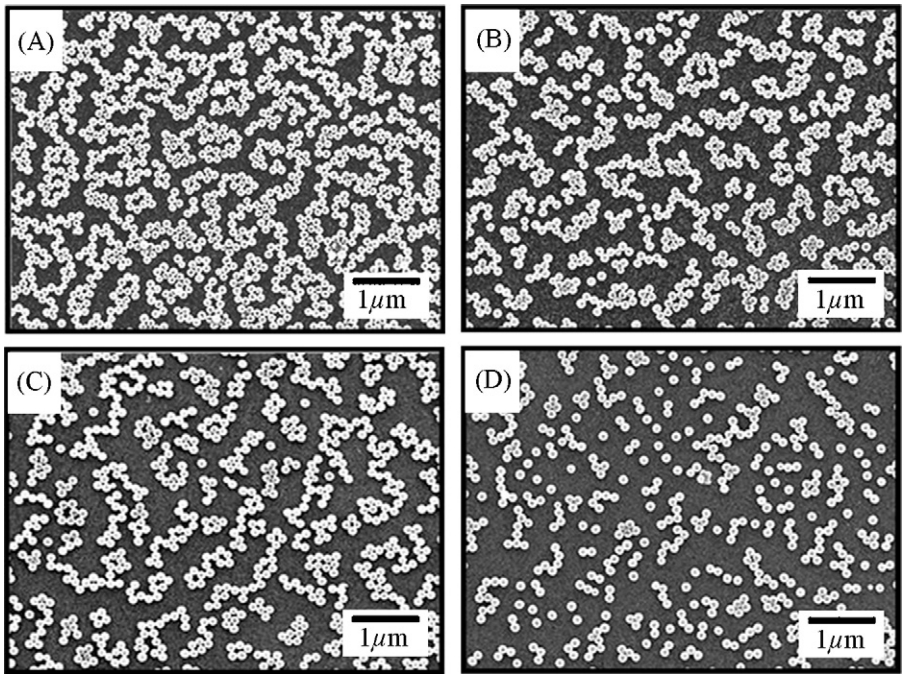

Fig. 3. SEM images showing pH-dependent results at room temperature for 2 h from the solution 1 at pH 2.0 (A), pH 3.0 (B), pH 4.0(C), and pH 5.6 (D), respectively.

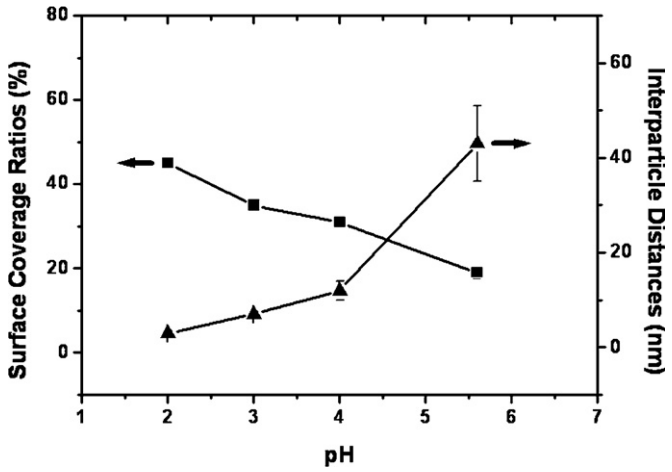

Fig. 4. Surface coverage ratios (–▲–) and interparticle distance (–■–) vs. reaction time showing coverage ratios decreased and interparticle distances increased as the pH increased.

of the initiator. Fig. 1 shows a schematic diagram of the experimental procedures for fabricating the colloidal monolayer through the self-assembly of PMMA particles on APTES-coated silicon substrate. Dipping of the APTES-coated substrates in a HCl solution and washing with distilled water allows not only an increase in the hydrophilicity of the substrate surface but also gives the substrates a positive charge, which enhances the electrostatic attraction with the negatively charged PMMA spheres. The weakly bounded PMMA on the substrate was removed by washing with deionized water before drying the samples.

3.1.1. Concentration and pH

The adhesion of the PMMA on the APTES modified substrate was examined by the particle coverage ratios, as summarized in Tables 1 and 2. Table 1 and Fig. 2 report the data obtained at different concentrations at room temperature. A higher solution concentration produced the larger coverage but less homogenous arrays than a lower concentration, for example, a 7% higher value resulted in an increase in the sedimentary colloidal particles. The capillary forces between the particles during the drying process induced the clustering of particles in solution 1 by overcoming the particle-substrate attractive interaction [16]. The sample prepared in solution 2 showed a non-close-packed structure with regular interparticle distances between the PMMA beads without the use of pre-patterned templates.

The pH-dependent assembly at room temperature was examined, and the results are shown in Figs. 3 and 4. Solution 3 with the lowest pH of 2.0 showed remarkably larger coverage ratios, more than double that of solution 1 (from 19% to 45%), indicating the formation of close packed PMMA. The small changes in pH from 3.0 to 2.0 altered the coverage significantly from 35% to 45%. The large decrease in interparticle distance from 96 nm to 76 nm was induced, as shown in Fig. 4. When the pH of the solutions was decreased, there was an increase in the level of protonation of the amine group of APTES, which enhanced the electrostatic attraction between the PMMA and APTES surface.

3.1.2. Reaction time and temperature

The influence of the reaction time on the particle assembly was investigated, as shown in Figs. 5 and 6. The surface coverage ratios increased from 12% to 22% as the dipping time was increased from 2 h to 18 h, presumably due to the increase in the population of sedimentary particles as a function of time [19]. As shown in Table 1, the results showed that the coverage ratios increased linearly with reaction time, where the 18 h sample of solution 3 showed 52% coverage. An increase in reaction time induced a significant decrease in the interparticle distance to 39 nm, compared with 152 nm for the 2 h-coated sample.

The reaction temperature is the other critical factor that influences monolayer assembly, as summarized in Fig. 7 and Table 2. Temperature is the predominant factor for obtaining high coverage ratios, i.e., solution 3 at 80 °C gave a value of 50%.

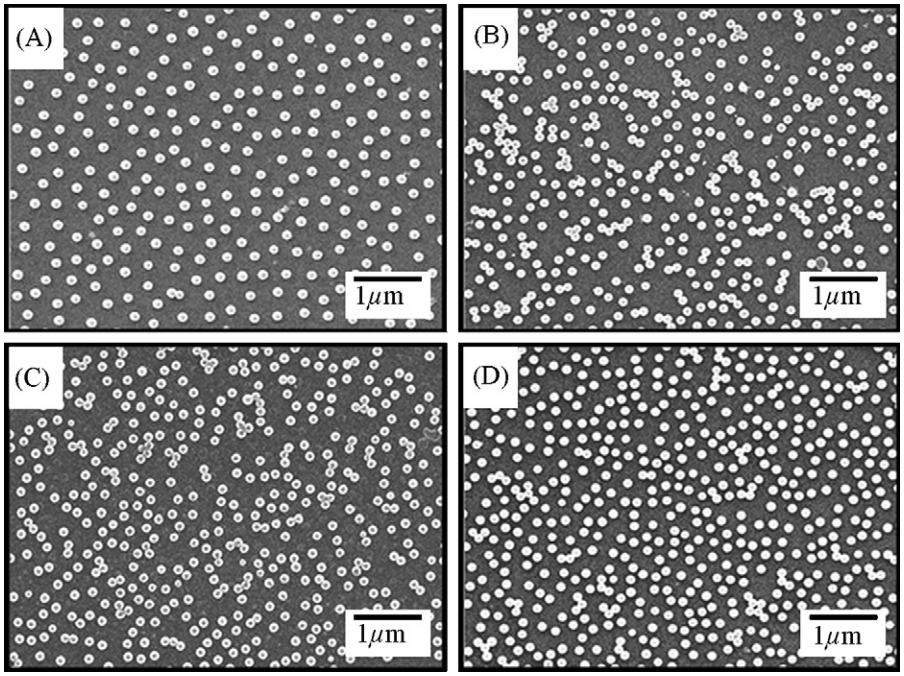

Fig. 5. SEM images showing the time-dependent change of the surface coverage ratios of the solution 2 at room temperature for (A) 2 h, (B) 8 h, (C) 12 h and (D) 18 h, respectively.

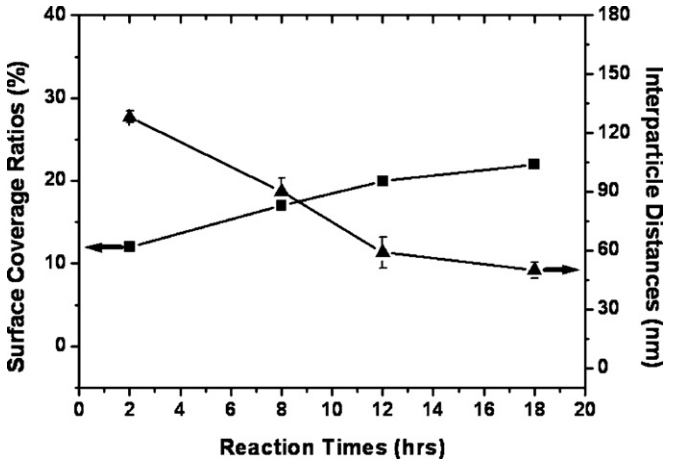

Fig. 6. Surface coverage ratios (–■–) and interparticle distance (–▲–) vs. reaction time showing coverage ratios increased and interparticle distances decreased as the dipping time increased.

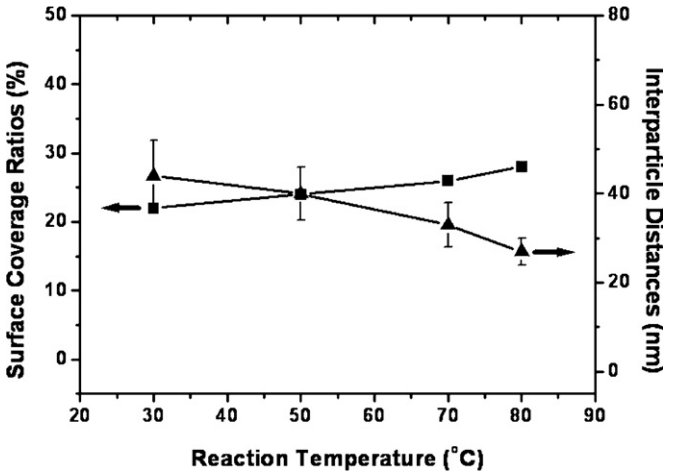

Fig. 8. Surface coverage ratios (–■–) and interparticle distance (–▲–) vs. reaction temperature showing the coverage ratios increased and interparticle distances decreased as the solution temperature increased.

Increasing the reaction temperature produced smaller interparticle distances than observed in the time-control experiments. At elevated temperatures, the defects of APTES-SAMs were filled by a rearrangement of the colloidal particles due to weakness of the adhesion strength as a result the thermal motion of the organic groups [20]. Fig. 8 shows the results for solution 2 as a function of temperature, where the coverage ratio increased up to 28% and the interparticle distances changed to 25 nm.

The driving forces for monolayer assembly are affected by Brownian motion, sedimentation rate and the type of the first ordered region formed by convective transport of the particles under the control of various experimental parameters, including the applied time, temperature and pH of the colloidal solutions [6]. It was found that temperature and pH are the main parameters in the present PMMA assembly. In particular, the deposition of colloidal particles at elevated temperatures caused the rearrangement of particles on the substrates, leading to regular particle arrays. The detailed SEM data are shown in the supporting data, Fig. S1-S3.

3.2. Fabrication of hemispherical Pt nanoshells

Hemispherical Pt nanoshells were prepared by thermal treatment after depositing Pt metal on the non-close-packed 2D PMMA monolayer as a template, which is comparable to the method using a pre-patterned substrate [21]. Fig. 9A–D show the plane- and cross-section SEM images of the structural transformation of the PMMA particles by the thermal treatments. The diameter of the PMMA area on the substrate was changed from 40 nm in the bulk state to 100 nm on the solid substrate.

Platinum deposition on PMMA and subsequent thermal treatment gave a nanoshell with spherical tops and nanosized cavities beneath the platinum layer. The Pt-coated PMMA were heated to 250 °C to remove the PMMA spheres, which led to the

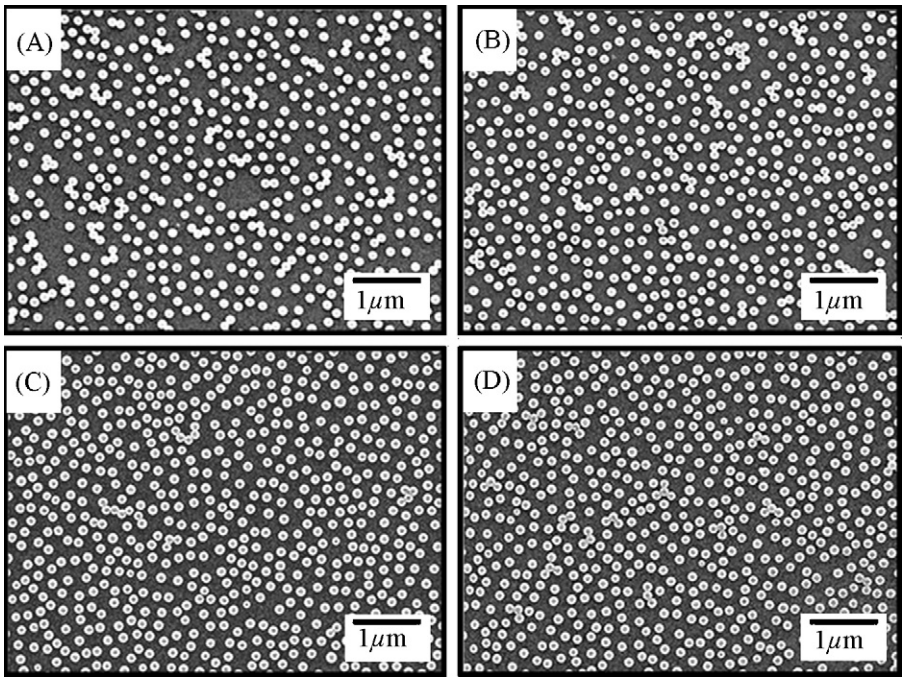

Fig. 7. SEM images showing the surface coverage ratios of the solution 2 for 2 h at elevated temperatures: 30 °C (A), 50 °C (B), 70 °C (C) and 80 °C (D), respectively.

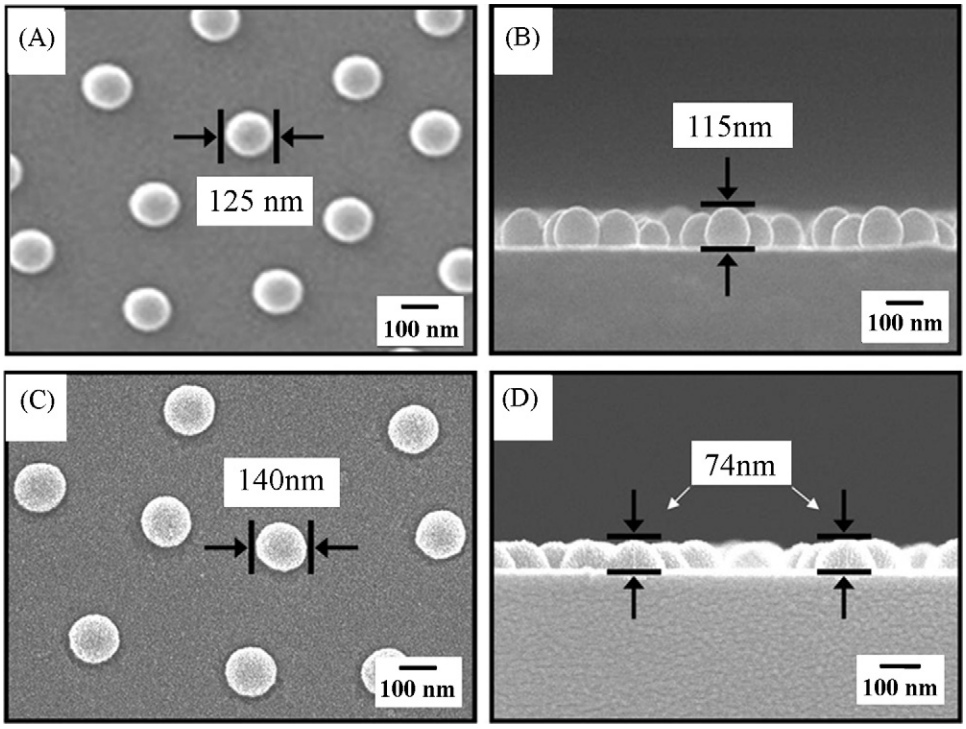

Fig. 9. The plane (A) and the cross-sectional (B) SEM images showing the sample made by solution 2 at 80 °C for 2 h. The particle diameter (*C*) increased and the height (*D*) decreased after thermal treatment at 250 °C.

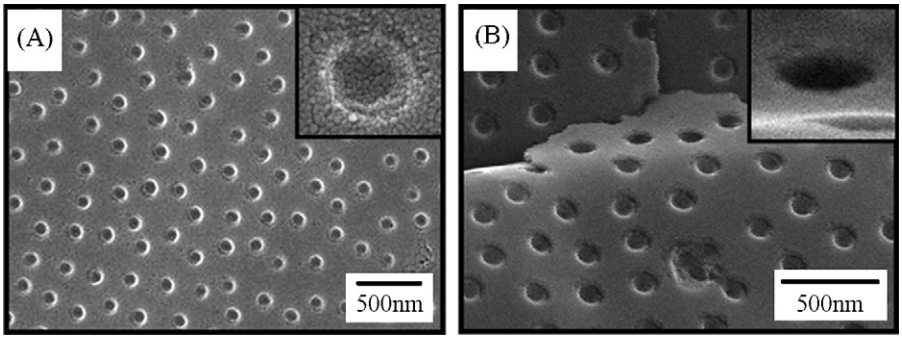

Fig. 10. The plane (A) and the cross-sectional (B) SEM images of the prepared hollow Pt nanoshell.

structural transformation of the Pt-PMMA composite from a spherical to hemispherical shape. The diameter of the hemisphere increased from 125 nm to 140 nm, and the contact angle of the Pt-PMMA composite on the APTES-coated substrate changed from 115° to 75°. The height of the Pt nanoshell decreased remarkably from 115 nm to 74 nm due to the absence of a Pt layer underneath the equator of the PMMA spheres during Pt sputtering.

Transfer of the hemispherical Pt nanoshell onto carbon tape allows an observation of the hollow interior of the nanoshell. Fig. 10 shows SEM images of the nanoshells. From the nanosized spherical wells, it was confirmed that the deposition of a thin layer of platinum produced a hollow architecture with nanopores, and the nanoshells were covered with aggregated platinum nanoparticles in the white rim of the spherical wells, which is clearly seen in the inset in Fig. 10A. Despite the deposition of a thin layer of platinum, the prepared hemispherical nanostructures were robust enough to resist temperatures up to 250 °C and subsequent transfer onto carbon tape.

4. Conclusions

The 2D array of the PMMA colloidal particles was optimized by adopting a coupling agent on the substrate to produce a strong electrostatic interaction between the substrate and the colloidal particles. Several experimental parameters, such as the dipping time, temperature and solution pH, were used to control the interparticle spacing of the adsorbed PMMA particles by temperature control. The highest surface coverage ratios were obtained at pH 2.0. Temperature had the most significant effect on the regular interparticle distances, which provided a template for fabricating hemispherical Pt nanoshells. Further experiments to change the colloidal crystal density and particle arrangement are currently underway. The present synthetic strategy will be expanded to building blocks for 3D photonic crystals through layer-by-layer assembly as well as to 2D templates for microembossed materials by molding.

Acknowledgements

This research was supported from the Brain Korea (BK) 21 program, the Korea Research Foundation Grant funded by Korean government (MOEHRD) (KRF-2005-005-J11902) and the National Research Laboratory Program of Korea Science and Engineering Foundation (Program No. ROA-2007-000-10020-0).

Appendix A. Supplementary data

Supplementary data associated with this article can be found, in the online version, at doi:10.1016/j.apsusc.2008.09.057.

References

[1] T. Okubo, A. Tsuchida, T. Tanahashi, A. Iwata, S. Okada, S. Kobata, K. Kobayashi, Colloids Surfaces A: Physicochem. Eng. Aspects 149 (1999) 431.
[2] J. Holtz, S.A. Asher, Nature 389 (1997) 829.
[3] Y.-J. Lee, P.V. Braun, Adv. Mater. 15 (2003) 563.
[4] T.R. Kline, W.F. Paxton, Y. Wang, D. Velegol, T.E. Mallouk, A. Sen, J. Am. Chem. Soc 127 (2005) 17150.
[5] K. Katagiri, M. Hashizume, J.-I. Kikuchi, Y. Taketani, M. Murakami, Colloids Surf. B: Biointerfaces 38 (2004) 149.
[6] Y. Xia, B. Gates, B.Y. Yin, Y. Lu, Adv. Mater. 12 (2000) 693.
[7] C. Lopez, Adv. Mater. 15 (2003) 1679.
[8] M. Geissler, Y. Xia, Adv. Mater. 16 (2004) 1249.
[9] H. Becker, C. Gärtner, Electrophoresis 21 (2000) 12.
[10] Y. Chen, Y. Pépin, Electrophoresis 22 (2001) 187.
[11] Y. Yin, Z.–Y. Li, Y. Xia, Langmuir 19 (2003) 622.
[12] Y. Xia, Y. Yin, Y. Lu, J. Mclellan, Adv. Funct. Mater. 13 (2003) 907.
[13] M.R. Böhmer, E.A. van der Zeeuw, G.J.M. Koper, J. Colloid Interface Sci. 197 (1998) 242.
[14] J. Schmitt, P. Mächtle, D. Eck, H. Mohwald, C.A. Helm, Langmuir 15 (1999) 3256.
[15] A. Walcarius, M. Etienne, B. Lebeau, Chem. Mater. 15 (2003) 2161.
[16] N.D. Denkov, O.D. Velev, P.A. Kralchevsky, I.B. Ivanov, H. Yoshimura, Langmuir 8 (1992) 3183.
[17] W. Dong, H.J. Bongard, F. Marlow, Chem. Mater. 15 (2003) 568.
[18] R.J. Hunter, Fundations of Colloid Science, 1, Oxford University Press, Oxford, 1986, p. 380.
[19] B.J. Tarasevich, P.C. Rieke, J. Liu, Chem. Mater. 8 (1996) 292.
[20] Y. Masuda, T. Sugiyama, W.S. Seo, K. Koumoto, Chem. Mater. 15 (2003) 2469.
[21] Y. Lu, Y. Yin, Y. Xia, Adv. Mater. 13 (2001) 34.